

An asymmetric and fast Rydberg gate protocol for long range entanglement

Daniel C. Cole,¹ Vikas Buchemavari,^{2,3} and Mark Saffman^{4,5}

¹*Inflection, Boulder, CO, 80301, USA*

²*Center for Quantum Information and Control, University of New Mexico, Albuquerque, 87131, NM, USA*

³*Department of Physics and Astronomy, University of New Mexico, Albuquerque, NM, 87106, USA*

⁴*Inflection, Madison, WI, 53703, USA*

⁵*Department of Physics, University of Wisconsin-Madison, 1150 University Avenue, Madison, WI, 53706 USA*

(Dated: December 30, 2025)

We analyze a new Rydberg gate design based on the original $\pi - 2\pi - \pi$ protocol [Jaksch, et. al. Phys. Rev. Lett. **85**, 2208 (2000)] that is modified to enable high fidelity operation without requiring a strong Rydberg interaction. The gate retains the $\pi - 2\pi - \pi$ structure with an additional detuning added to the 2π pulse on the target qubit. The protocol reaches within a factor of 2.39 (1.68) of the fundamental fidelity limit set by Rydberg lifetime for equal (asymmetric) Rabi frequencies on the control and target qubits. We generalize the gate protocol to arbitrary controlled phases. We design optimal target-qubit phase waveforms to generalize the gate across a range of interaction strengths and we find that, within this family of gates, the constant-phase protocol is time-optimal for a fixed laser Rabi frequency and tunable interaction strength. Robust control methods are used to design gates that are robust against variations in Rydberg Rabi frequency or interaction strength.

I. INTRODUCTION

The strong interaction of Rydberg atoms provides a mechanism for entangling neutral atom qubits as was originally proposed in Ref. [1] using a $\pi - 2\pi - \pi$ sequence of ground-Rydberg pulses. The original protocol was first demonstrated in Refs. [2, 3], but has since been supplanted by improved protocols that apply the same optical pulses symmetrically to both atoms [4–10]. The symmetric protocols simplify optical control requirements and use of a time-optimal protocol has led to CZ fidelities surpassing $\mathcal{F} = 0.993$ with four different atomic species: Rb [11], Cs [12], Sr [13], and Yb [14–16]. While high fidelity is critical for quantum error correction, leveraging the long range nature of the Rydberg interaction is also of interest for implementing non-local error correcting codes [17, 18].

We present here a modified version of the $\pi - 2\pi - \pi$ gate that has the remarkable feature of having no coherent rotation error (that is, it achieves unity fidelity in the absence of dissipation and experimental imperfections), even in the partial blockade limit of interaction strength V comparable to Rydberg excitation rate Ω . The ability to provide high fidelity for moderate V implies that the gate can be operated at large inter-atomic spacings.

We proceed in Sec. II by briefly reviewing the original $\pi - 2\pi - \pi$ protocol shown in Fig. 1 and the associated gate fidelity analysis. In Sec. III we describe the new protocol, provide a simplified error analysis, and generalize the gate for arbitrary controlled phases. We generalize the protocol to different interaction strengths using optimal control in Sec. IV. An enhanced asymmetric protocol that uses phase-modulated pulses on the target qubit to achieve robustness against variations in Rabi frequency and interaction energy is analyzed in Sec. V. We conclude with a comparison of the new protocol relative to fundamental limits in Sec. VI.

II. $\pi - 2\pi - \pi$ RYDBERG GATE

The original Rydberg CZ gate protocol [1] is based on a three pulse sequence. A π pulse is applied to the control qubit, a 2π pulse is applied to the target qubit, and a final π pulse is applied to the control qubit. Each pulse is resonant with the $|0\rangle \leftrightarrow |r\rangle$ transition^a where the qubit basis is $|0\rangle, |1\rangle$ and $|r\rangle$ is the Rydberg state. In the idealized limit of $V, \omega_q \gg \Omega \gg 1/\tau$ where V is the two-atom interaction strength, ω_q is the energy separation of $|0\rangle$ and $|1\rangle$, Ω is the ground-Rydberg Rabi frequency, and τ is the Rydberg lifetime we obtain the mapping for control, target basis states $|ct\rangle$:

$$|00\rangle \rightarrow -e^{-i\phi_{00}} |00\rangle, \quad (1a)$$

$$|01\rangle \rightarrow -e^{-i\phi_{01}} |01\rangle, \quad (1b)$$

$$|10\rangle \rightarrow -e^{-i\phi_{10}} |10\rangle, \quad (1c)$$

$$|11\rangle \rightarrow e^{-i\phi_{11}} |11\rangle. \quad (1d)$$

Here $\phi_{00}, \phi_{01}, \phi_{10}, \phi_{11}$ are dynamical phases from differential Stark shifts on the qubit states due to the Rydberg pulses and the minus signs on the first three states are geometrical phases from the trajectory with area 2π in the $\{|0\rangle, |r\rangle\}$ Hilbert space. When all three pulses use the same Rabi rate the dynamical phases can be expressed as $\phi_{00} = 2\phi_0$, $\phi_{01} = \phi_{10} = \phi_0 + \phi_1$, $\phi_{11} = 2\phi_1$, with ϕ_0, ϕ_1 the single atom Stark shifts on states $|0\rangle, |1\rangle$ during the gate. Applying a global phase rotation $R_z(\phi_1 - \phi_0) \otimes R_z(\phi_1 - \phi_0)$ and suppressing an irrelevant global phase we obtain the canonical CZ gate:

$$|00\rangle \rightarrow |00\rangle, \quad (2a)$$

$$|01\rangle \rightarrow |01\rangle, \quad (2b)$$

$$|10\rangle \rightarrow |10\rangle, \quad (2c)$$

$$|11\rangle \rightarrow -|11\rangle. \quad (2d)$$

^a We adopt this convention to simplify phase calculations.

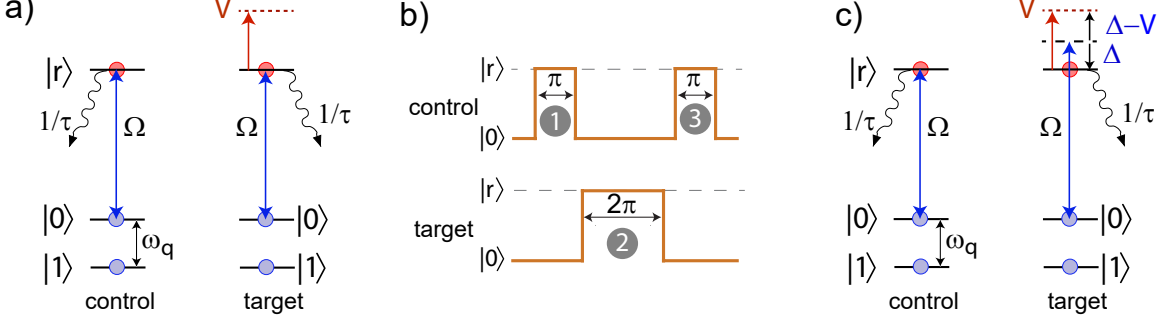


FIG. 1. Protocol for a Rydberg CZ gate. a) Atomic levels with qubits encoded in $|0\rangle, |1\rangle$ that are separated by ω_q . State $|0\rangle$ is coupled to $|r\rangle$ with Rabi frequency Ω . The Rydberg levels decay at rate $1/\tau$ and the two-atom interaction strength is V . b) A three pulse gate protocol is: 1) π pulse on control qubit, 2) 2π pulse on target, 3) π pulse on control. c) A modified gate protocol is the same as in a) and b) except that the 2π pulse on the target is detuned by Δ .

In practice the ratios V/Ω and $\Omega/(1/\tau)$ are chosen to be large but finite, while $\omega_q \gg V$. This leads to the dominant error terms being those due to decay from the Rydberg state and incomplete blocking of the target atom rotation when the control atom is Rydberg excited. The errors are minimized by choosing the Rabi frequency to be $\Omega_{\text{opt}} = (7\pi)^{1/3} (V^2/\tau)^{1/3}$ which leads to a minimum gate error of [19]:

$$\epsilon_{\pi-2\pi-\pi} = \frac{3(7\pi)^{2/3}}{8} \frac{1}{(V\tau)^{2/3}}. \quad (3)$$

Note that the minimum error scales as $\epsilon_{\pi-2\pi-\pi} \sim (V\tau)^{-2/3}$ whereas the best possible scaling for an arbitrary gate protocol is $\epsilon_{\text{DDP}} = (1 + \pi/2)/(V\tau) \simeq 2.57/(V\tau)$ [20, 21].

The highest fidelity that has been demonstrated with the $\pi - 2\pi - \pi$ gate is $\mathcal{F} = 1 - \epsilon = 0.89$ [22]. Detailed numerical analysis taking into account the finite spacing of Rydberg levels in Rb and Cs atoms [23] leads to an error floor in the absence of technical imperfections that is at best $\epsilon \simeq 0.002$. This can be improved on by using shaped pulses to suppress excitation of neighboring Rydberg states in which case errors as low as $\epsilon < 10^{-4}$ are theoretically achievable, albeit with the requirement of very fast Rydberg pulses and very strong interactions [24].

III. ASYMMETRIC $\pi - 2\pi - \pi$ RYDBERG GATE

The error scaling of the gate can be improved by detuning the pulse on the target atom by an amount $\Delta = \omega - \omega_{r0}$ where ω is the laser frequency and ω_{r0} is the atomic ground-Rydberg frequency. With this detuning the $|10\rangle$ state will return to the ground state provided

$$t\sqrt{|\Omega|^2 + \Delta^2} = 2\pi \quad (4)$$

and the $|00\rangle$ state will return to the ground state provided

$$t\sqrt{|\Omega|^2 + (\Delta - V)^2} = 2\pi. \quad (5)$$

Here we assume Δ and V are the same sign. In both cases we can achieve full return of the target atom to the ground state (neglecting Rydberg scattering) provided $\Delta = V/2$ and $t = 2\pi/\sqrt{|\Omega|^2 + V^2/4}$. The amplitude factor imparted by the 2π pulse on the target atom when the control atom is not (is) excited is $e^{-i\phi_V}$ with

$$\phi = \pi + \frac{\Delta t}{2} = \pi + \frac{\pi\Delta}{\sqrt{|\Omega|^2 + \Delta^2}}, \quad (6a)$$

$$\phi_V = \pi + \frac{(\Delta - V)t}{2} = \pi + \frac{\pi(\Delta - V)}{\sqrt{|\Omega|^2 + (\Delta - V)^2}}. \quad (6b)$$

Choosing $\Omega = \sqrt{3}V/2$ and $t = 2\pi/V$, we find $\phi = 3\pi/2$, $\phi_V = \pi/2$. The gate mapping on $|ct\rangle$ is

$$|00\rangle \rightarrow -e^{i(-\pi/2 - \phi_{0c} - \phi_{0t})} |00\rangle, \quad (7a)$$

$$|01\rangle \rightarrow -e^{-i(\phi_{0c} + \phi_{1t})} |01\rangle, \quad (7b)$$

$$|10\rangle \rightarrow -e^{i(-\pi/2 - \phi_{1c} - \phi_{0t})} |10\rangle, \quad (7c)$$

$$|11\rangle \rightarrow e^{-i(\phi_{1c} + \phi_{1t})} |11\rangle \quad (7d)$$

where $\phi_{0c/t}$ is the dynamical phase on state $|0\rangle$ for the control/target atoms and similarly for state $|1\rangle$. These phases are no longer identical for the control and target since the Rydberg pulse on the target atom is detuned. Applying single qubit rotations $R_z(\phi_{1c} - \phi_{0c}) \otimes R_z(-\pi/2 + \phi_{1t} - \phi_{0t})$ we obtain up to a global phase the canonical CZ gate of Eqs. (2).

Even though the interaction strength is finite, $V = 2\Omega/\sqrt{3}$, there is no rotation error. To leading order the error is only due to Rydberg scattering. The integrated population in the Rydberg state, averaged over the computational basis states, is $P_r = \pi(33 + 8\sqrt{3})/(24V)$ which gives a scattering error of

$$\epsilon = \frac{P_r}{\tau} = \left(\frac{11}{8} + \frac{1}{\sqrt{3}} \right) \frac{\pi}{V\tau} \simeq 2.39 \times \epsilon_{\text{DDP}}. \quad (8)$$

We see that the asymmetric gate protocol reaches within a factor of about three of the error limit.

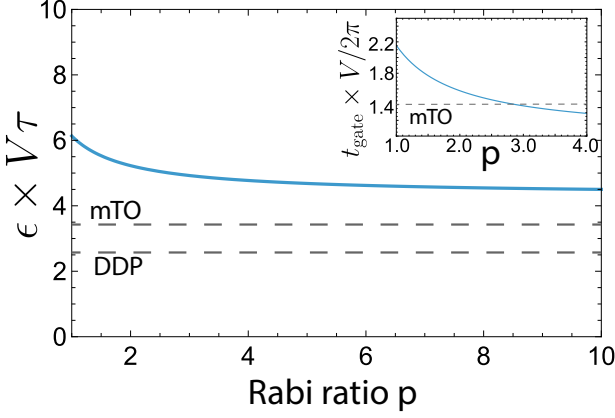


FIG. 2. Rydberg-scattering-limited gate error for the asymmetric protocol with $\Omega_c = p\Omega$. The dashed line labeled DDP shows the bound of $\epsilon_{\text{DDP}}V\tau = 2.57$ from [21] and the line labeled mTO is the modified time optimal gate of Ref. [17], Table II, gate 11. The inset shows the gate duration for the asymmetric and the modified time-optimal gates.

We can reach closer to the error limit with a simple modification to the protocol by driving the target atom with Rabi rate Ω and the control atom with Rabi rate $\Omega_c = p\Omega$, allowing for $p > 1$. Since the control atom is not subject to blockade p may be arbitrarily large up to practical limits set by available laser power and coupling to neighboring Rydberg states [24]. We then find

$$\epsilon = \left(\frac{11}{8} + \frac{1}{\sqrt{3}p} \right) \frac{\pi}{V\tau} \rightarrow \frac{11\pi}{8} \frac{1}{V\tau} \text{ for } p \rightarrow \infty. \quad (9)$$

The gate duration is

$$t_{\text{gate}} = \left(1 + \frac{2}{\sqrt{3}p} \right) \frac{2\pi}{V} \rightarrow \frac{2\pi}{V} \text{ for } p \rightarrow \infty. \quad (10)$$

The error and gate duration are plotted in Fig. 2. At $p = 1$ the error is $\epsilon = 2.39\epsilon_{\text{DDP}}$ and the limit of $p \rightarrow \infty$ gives $\epsilon_{\min} = 1.68\epsilon_{\text{DDP}}$ for the asymmetric gate. For comparison we note that the adiabatic Rydberg dressing gate [25] achieves $\epsilon/\epsilon_{\text{DDP}} = 2.45$, the modified time-optimal gate [17] achieves $\epsilon/\epsilon_{\text{DDP}} = 1.33$, and the interaction gate [1] in the limit of rapid excitation of both atoms to the Rydberg state achieves $\epsilon/\epsilon_{\text{DDP}} = 1.22$. Thus the fidelity of the asymmetric gate introduced here is comparable to previous designs.

A. Generalizations

The asymmetric protocol may also be used to implement a general phase gate with the mapping $U = \text{diag}[1, 1, 1, e^{i\theta}]$ by adjusting the Rabi frequency Ω as $\Omega = V \cdot \sqrt{(\pi/\theta)^2 - 1/4}$. The target qubit pulse duration is adjusted accordingly to $t = 2\theta/V$. Extending the target qubit pulse duration to $2n\theta/V$ produces a controlled

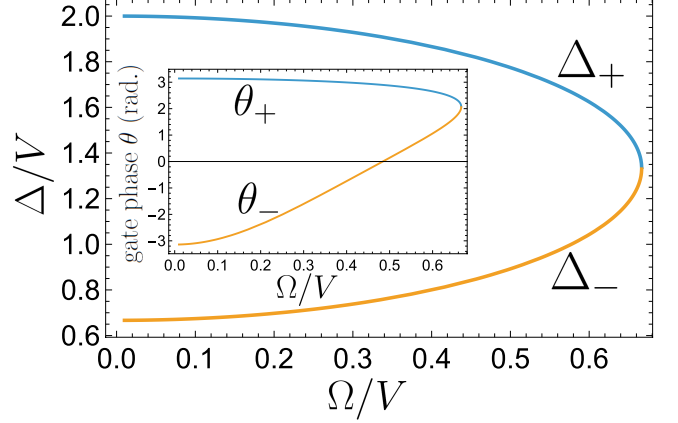


FIG. 3. General phase gate dependence on Rabi rate Ω from solutions of Eq. (13) for $n_1 = 2, n_2 = 1$. The inset shows the corresponding gate phase.

$n\theta$ gate in which the state of the target qubit traverses n loops on the $|0\rangle - |r\rangle$ Bloch sphere.

Controlled phase gates can also be constructed for values of the detuning other than $\Delta = V/2$. In this case the detuning, Rabi frequency, and duration must be chosen so that n_0 (n_V), the number of Bloch-sphere loops traversed by the target qubit state in the absence (presence) of the Rydberg interaction, is an integer. We satisfy Eqs. (4,5) at multiple 2π rotations as

$$t\sqrt{|\Omega|^2 + \Delta^2} = 2\pi n_0 \quad (11)$$

$$t\sqrt{|\Omega|^2 + (\Delta - V)^2} = 2\pi n_V. \quad (12)$$

with n_0, n_V integers. This leads to solutions for $n_0 \neq n_V$:

$$\Delta_{\pm} = \frac{n_0^2 V \pm [n_0^2 n_V^2 V^2 - (n_0^2 - n_V^2)^2 \Omega^2]^{1/2}}{n_0^2 - n_V^2}. \quad (13)$$

The target atom phases corresponding to Eqs. (6) are then given by

$$\phi_{\pm} = n_0\pi + \frac{n_0\pi\Delta_{\pm}}{\sqrt{|\Omega|^2 + \Delta_{\pm}^2}}, \quad (14)$$

$$\phi_{V,\pm} = n_V\pi + \frac{n_0\pi(\Delta_{\pm} - V)}{\sqrt{|\Omega|^2 + \Delta_{\pm}^2}}, \quad (15)$$

and the gate phase is

$$\theta_{\pm} = \phi_{V,\pm} - \phi_{\pm}. \quad (16)$$

An example showing that θ can be tuned over the full range from $-\pi$ to π is given in Fig. 3.

IV. TIME-OPTIMAL PULSE DESIGNS

By allowing a time-varying Rydberg laser phase during the target-qubit pulse, a general family of gates is

Fixed parameter	Ω	V
Analytic gate is optimal	Globally	Locally
Limit	$V \rightarrow \infty$	$\Omega \rightarrow \infty$
Asymptotic duration	$2\pi/\Omega$	π/V
Asymptotic classification	$\pi - 2\pi - \pi$ gate	Interaction gate
Duration of analytic gate	$\sqrt{3}\pi/\Omega$	$2\pi/V$

TABLE I. A comparison of the duration of the analytic, constant-Rydberg-phase gate to asymptotic gates. We take $p \rightarrow \infty$, which has no impact on target-qubit dynamics and only affects total gate duration. The analytic gate is time-optimal when Ω is fixed and V may be varied. It is locally optimal for fixed V and variable Ω , but longer than the interaction gate in the limit $\Omega \rightarrow \infty$.

obtained. We explore gates in this family using Gradient Ascent for Pulse Engineering (GRAPE) [26] to optimize a piecewise-constant Rydberg laser phase ξ during the target atom pulse, similar to optimizations [8, 9] for the Levine-Pichler gate [6]. We first explore time-optimal solutions for the laser phase as the ratio Ω/V is varied, and in the next section we present robust pulse designs.

We use a binary search algorithm to find the shortest duration at which the error is below a target value (in the absence of decay mechanisms), which we set to be 10^{-8} [27]. We do not include Rydberg decay in the dynamics for gate optimization as it does not make an appreciable difference in the optimal gate durations and waveforms [8, 28]. Results of this optimization are shown in Fig. 4. For simplicity we describe gate durations in the limit $p \rightarrow \infty$, with $p = \Omega_c/\Omega$ as defined above. We consider notable limiting cases: First, if V is fixed and Ω can be varied, the gate duration approaches $\tau = \pi/V$ as $\Omega \rightarrow \infty$. In this limit the gate dynamics resemble the interaction gate, in which the target qubit in $|00\rangle$ (which is excited to $|r0\rangle$ by the first control-qubit pulse) and in $|10\rangle$ is rapidly excited to the Rydberg state, the state is allowed to evolve for a time τ , then the target qubit is rapidly de-excited. The free evolution can be achieved by setting $\Omega = 0$; in our fixed- Ω optimization, the free evolution is achieved via detuning modulations, as shown in Fig. 4b.

Second, if Ω is fixed and V is varied, then the gate duration asymptotically approaches $2\pi/\Omega$ as $V \rightarrow \infty$; this is the original $\pi - 2\pi - \pi$ gate [1]. Table I presents a comparison of these limiting cases with the analytic gate discussed above. We find that, within the family of gates considered here, an interaction strength of $V = 2\Omega/\sqrt{3}$ optimally makes use of fixed available Rabi frequency for a duration of $\tau = 5.441/\Omega$ (see Fig. 4a inset). This point also yields the time-optimal atomic separation for a fixed Rabi frequency. Similar speedups at moderate interaction strength have been observed in other Rydberg gates [28, 29]. An important caveat is that taking the limit $p \rightarrow \infty$ invalidates direct comparison to the time-optimal symmetrically addressed gate, which achieves total duration of $\tau = 7.612/\Omega$ in the limit $V \rightarrow \infty$.

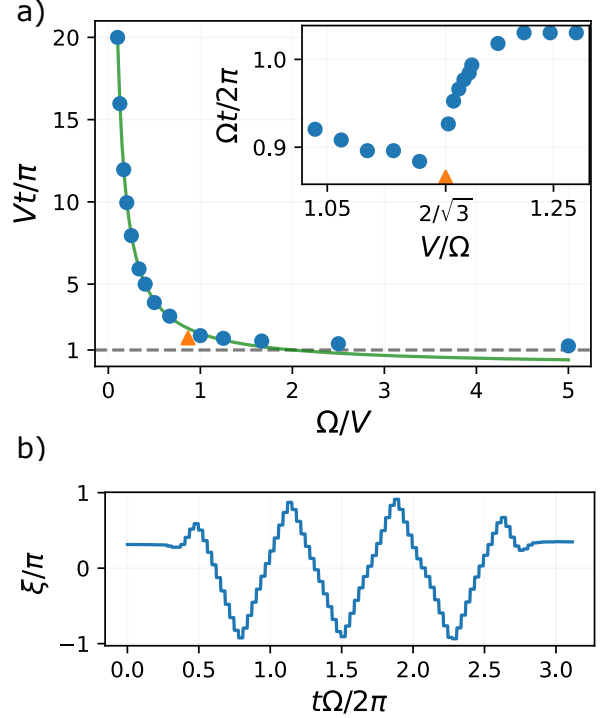


FIG. 4. Time-optimal solutions for the target pulse as the ratio Ω/V is varied. (a) GRAPE-optimized target pulse duration as a function of Rabi frequency Ω/V for a fixed interaction strength V . The limiting durations $\tau = 2\pi/\Omega$ and $\tau = \pi/V$ discussed in the main text are shown by solid green and dashed grey lines, respectively. The duration of the analytic gate is shown by the orange triangle. Inset: Gate duration for fixed Ω as V is varied. In this case the analytic gate is the global minimum. (b) Optimized gate waveform for $\Omega/V = 5$, for which dynamics approximate the limit $\Omega \rightarrow \infty$. This waveform approximates the interaction gate and achieves effective free evolution with large detunings; here $|\Delta|_{\max} \approx 2.5\Omega$.

V. ROBUST PULSE DESIGNS

In addition to optimizing gate speed for a fixed set of parameters, quantum control techniques can be employed to design robust gates. Here we consider gates that maintain high fidelity despite static but unknown errors in specific parameters. We use robust control to design gates that are resilient to variations in Rabi frequency Ω and interaction strength V . The optimization is performed at $\Omega = \sqrt{3}V/2$ and we assume $p \rightarrow \infty$ to simplify the numerics.

Modifying the phase waveform of the pulse on the target qubit to obtain a robust gate inevitably requires an increase in the duration of the pulse relative to the time-optimal case, and the integrated Rydberg population increases accordingly. Therefore, finding concrete solutions requires assigning values to the Rydberg lifetime and to the scale of the variation to which robustness is desired. In our studies we take as a representative example

$\Omega/\Gamma = 2\pi \times 150$, where Γ is the decay rate out of the Rydberg state; this ratio roughly corresponds e.g. to $\Omega/2\pi = 1$ MHz and $\Gamma = 1/143\ \mu\text{s}$ for Rydberg principal quantum number $n = 70$ in ^{133}Cs at $T = 300$ K [30]. Robustness against variation of a noisy Hamiltonian parameter with nominal value q is obtained by optimizing the phase-modulation vector $\vec{\xi}$ to maximize the quantity $2\mathcal{F}(q) + \mathcal{F}(0.95q) + \mathcal{F}(1.05q)$ (other gate parameters are stable and are suppressed as arguments for simplicity), where we have chosen a 5 % scale of variation for optimization [10, 28, 31].

Fig. 5 summarizes optimization for robustness against Rabi frequency variation. We find that the gate duration that provides the optimal compromise between minimization of fidelity variation over $\pm 5\%$ and minimization of Rydberg-decay error is $t \approx 2t_{\text{opt}}$, with $t_{\text{opt}} = 2\pi/V$ for the analytic gate. As the ratio Ω/Γ increases, the optimal gate duration relative to $2\pi/\Omega$ increases and robustness improves [13]. To further quantify robustness, we define an average weighted gate error over a Gaussian distribution of Rabi frequencies Ω , centered at Ω_0 , with variance σ^2 :

$$1 - \bar{\mathcal{F}} = \int p(\Omega)(1 - \mathcal{F}(\Omega))d\Omega \quad (17)$$

$$p(\Omega) = \frac{1}{\sqrt{2\pi\sigma^2}} \exp\left[-\frac{1}{2}\left(\frac{\delta\Omega/\Omega_0}{\sigma}\right)^2\right]. \quad (18)$$

Figure 5c depicts the dependence of this error on the gate duration.

Fig. 6 summarizes optimization for robustness against variation in the interaction strength V . Due to the dependence of the Rydberg interaction on inter-atomic distance as $V = r^{-\alpha}$ with $\alpha = 3$ (dipole-dipole interaction) or $\alpha = 6$ (van der Waals interaction), interaction can vary strongly for realistic noise in the inter-atomic separation. This is especially impactful in the regime where $\Omega \sim V$, as gate dynamics are much more sensitive to the particular ratio Ω/V than in the limit $V \rightarrow \infty$ where double excitation to $|RR\rangle$ is strongly suppressed over a wide range of values V . With $\delta V/V \approx -\alpha\delta r/r$, one finds for example that for atoms separated by 6 microns, a plausible 50 nm spacing error (as may arise from finite temperatures in optical tweezers) produces $\delta V/V \approx 5\%$. For optimization against this variation with $\Omega/\Gamma = 2\pi \times 150$, we find the optimal duration to be $t \approx 1.5t_{\text{opt}}$, at which the gate error is reduced threefold at 5 % interaction-strength error.

VI. DISCUSSION

A wide range of Rydberg gate protocols have been proposed and implemented, although only a few of them have a gate error that scales as $1/(V\tau)$. The two-atom dark state gate [32] reaches $\epsilon = 14.8\epsilon_{\text{DDP}}$. The time-optimal gate reaches $\epsilon = 11.7\epsilon_{\text{DDP}}$ for the parameters

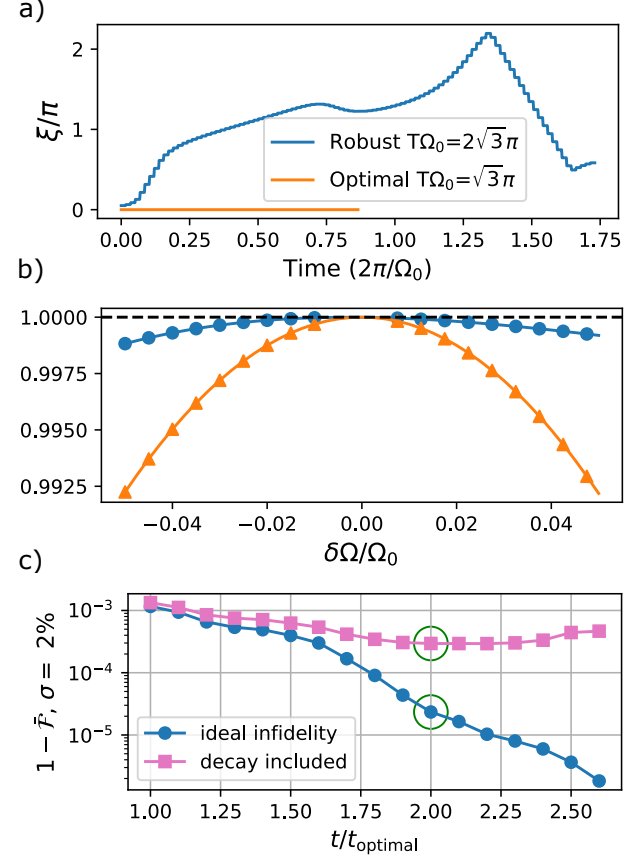


FIG. 5. Properties of target atom phase waveforms for a CZ gate designed to be robust against Rabi frequency fluctuations. a) The phase waveform for the analytic (orange, flat), and robust (blue) pulses. The robust pulse is twice as long as the analytic pulse and exhibits significant phase modulation. The maximal detuning corresponds to $|\Delta|_{\text{max}} \approx 2\Omega_0$. b) Gate fidelity without Rydberg decay as a function of fractional Rabi frequency error ($\delta\Omega/\Omega_0$) for both pulses. The robust pulse maintains high fidelity across the full $\pm 5\%$ range, with roughly sevenfold reduction in gate error at the extremes. c) Average gate error as a function of gate duration for Rabi-frequency-robust control, for normally distributed Rabi errors as described in the main text with $\sigma = 2\%$. As the gate duration increases, robust control achieves lower average gate error (Eq. 17) in the absence of decay (blue circles). The improvement is reduced when Rydberg decay is included (pink squares). At $t/t_{\text{optimal}} = 2$ (shown in green circles), the gain from robustness is balanced by error from decay, resulting in a plateau followed by an eventual rise in gate error.

analyzed in Ref. [8]. It was shown in Ref. [17] that modifying the time-optimal profile by smoothly apodizing the sinusoidal phase variation could reach an error as low as $\epsilon = 1.33\epsilon_{\text{DDP}}$. The protocol analyzed here reaches $\epsilon = 2.39\epsilon_{\text{DDP}}$ for equal Rabi frequencies on control and target atoms and $\epsilon = 1.68\epsilon_{\text{DDP}}$ when the control atom Rabi rate is much higher than that on the target atom.

An additional feature of the asymmetric gate is that it is both fast and long range due to the ability to reach

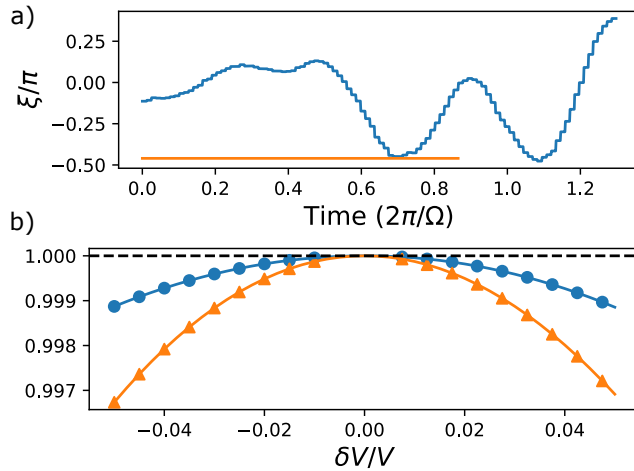


FIG. 6. Properties of target atom phase waveforms for a CZ gate designed to be robust against interaction strength fluctuations. a) The phase waveform for the analytic (orange, flat), and robust (blue) pulses. The robust pulse is 50% longer than the analytic pulse and exhibits significant phase modulation, with a maximum instantaneous detuning of $|\Delta|_{\max} \approx 2.8 \times \Omega$. b) Gate fidelity as a function of fractional interaction strength error ($\delta V/V$) for both pulses. The Robust pulse maintains higher fidelity across the full $\pm 5\%$ range, with roughly three-fold reduction in gate error at the extremes.

high fidelity with $\Omega \sim V$. In terms of the Rabi frequency the duration of the gate is $t_{\text{gate}}\Omega = \sqrt{3}\pi + 2\pi/p$. For $p = 1$ this is about 50% slower than the time-optimal gate, which requires $t_{\text{gate}}\Omega \simeq 7.6$ [8], but it is faster than the modified time-optimal gate for $p \geq 2.9$ (see Fig. 2). The operating distance of the gate can be characterized by the error scaling relative to ϵ_{DDP} , as a smaller scaling prefactor yields similar error at larger distance.

The range of the asymmetric gate is larger than that of the time-optimal gate and similar to that of the modified time-optimal gate. Relaxation of the requirement of strong blockade facilitates logical two-qubit gates [33] and quantum memory based on non-local low density parity check codes without atom motion [17, 18].

On the other hand gates that do not operate with strong blockade are intrinsically less robust to variations in atom spacing and interaction strength, as well as being susceptible to force-induced heating due to double-excitation to $|rr\rangle$. As has been discussed elsewhere (see Eq. (45) in [7]) the gate error arising from forces between doubly-excited states scales as $T_a V^2 P_{rr}^2 / (R^2 \omega^2)$. Here T_a is the atomic temperature, R is the atomic separation, P_{rr} is the integrated $|rr\rangle$ population, and ω is the trap vibrational frequency along the interatomic coordinate. Although this error can be reduced by increasing ω , doing so increases the errors due to photon recoil. Full optimization of gate parameters is a constrained problem that is dependent on the actual physical implementation, and is outside the scope of this work.

Finally we note that the asymmetric protocol presented here was demonstrated with Cs atoms as reported in [34]. The $66s_{1/2}$ level was excited using a two-photon approach with atoms spaced by $R \sim 6 \mu\text{m}$ giving an interaction strength of $V = 2\pi \times 6 \text{ MHz}$. A gate fidelity as high as 0.964 was achieved, likely limited by technical errors due to laser noise and finite atom temperature.

VII. ACKNOWLEDGMENTS

VB thanks Ivan H. Deutsch for fruitful discussions and support throughout this project. VB also acknowledges support from the Quantum New Mexico Institute (QNM-I).

[1] D. Jaksch, J. I. Cirac, P. Zoller, S. L. Rolston, R. Côté, and M. D. Lukin, Fast quantum gates for neutral atoms, *Phys. Rev. Lett.* **85**, 2208 (2000).

[2] L. Isenhower, E. Urban, X. L. Zhang, A. T. Gill, T. Henage, T. A. Johnson, T. G. Walker, and M. Saffman, Demonstration of a neutral atom controlled-NOT quantum gate, *Phys. Rev. Lett.* **104**, 010503 (2010).

[3] X. L. Zhang, L. Isenhower, A. T. Gill, T. G. Walker, and M. Saffman, Deterministic entanglement of two neutral atoms via Rydberg blockade, *Phys. Rev. A* **82**, 030306(R) (2010).

[4] Y. Sun, P. Xu, P.-X. Chen, and L. Liu, Controlled phase gate protocol for neutral atoms via off-resonant modulated driving, *Phys. Rev. Applied* **13**, 024059 (2020).

[5] M. Saffman, I. I. Beterov, A. Dalal, E. J. Paez, and B. C. Sanders, Symmetric Rydberg controlled- Z gates with adiabatic pulses, *Phys. Rev. A* **101**, 062309 (2020).

[6] H. Levine, A. Keesling, G. Semeghini, A. Omran, T. T. Wang, S. Ebadi, H. Bernien, M. Greiner, V. Vuletić, H. P. Büchler, and M. D. Lukin, High-fidelity parallel entangling gates on a neutral-atom quantum computer, *Nature* **590**, 509 (2021).

[7] F. Robicheaux, T. Graham, and M. Saffman, Photon recoil and laser focusing limits to Rydberg gate fidelity, *Phys. Rev. A* **103**, 022424 (2021).

[8] S. Jandura and G. Pupillo, Time-optimal two- and three-qubit gates for Rydberg atoms, *Quantum* **6**, 712 (2022).

[9] A. Pagano, S. Weber, D. Jaschke, T. Pfau, F. Meinert, S. Montangero, and H. P. Büchler, Error budgeting for a controlled-phase gate with Strontium-88 Rydberg atoms, *Phys. Rev. Res.* **4**, 033019 (2022).

[10] M. Mohan, R. de Keijzer, and S. Kokkelmans, Robust control and optimal Rydberg states for neutral atom two-qubit gates, *Phys. Rev. Res.* **5**, 033052 (2023).

[11] S. J. Evered, D. Bluvstein, M. Kalinowski, S. Ebadi, T. Manovitz, H. Zhou, S. H. Li, A. A. Geim, T. T. Wang, N. Maskara, H. Levine, G. Semeghini, M. Greiner, V. Vuletić, and M. D. Lukin, High-fidelity parallel entangling gates on a neutral-atom quantum computer, *Nature* **590**, 509 (2021).

622, 268 (2023).

[12] A. G. Radnaev, W. C. Chung, D. C. Cole, D. Mason, T. G. Ballance, M. J. Bedalov, D. A. Belknap, M. R. Berman, M. Blakely, I. L. Bloomfield, P. D. Buttler, C. Campbell, A. Chopinaud, E. Copenhaver, M. K. Dawes, S. Y. Eubanks, A. J. Friss, D. M. Garcia, J. Gilbert, M. Gillette, P. Goiporia, P. Gokhale, J. Goldwin, D. Goodwin, T. M. Graham, C. Guttormsson, G. T. Hickman, L. Hurtley, M. Iliev, E. B. Jones, R. A. Jones, K. W. Kuper, T. B. Lewis, M. T. Lichtman, F. Majdeteimouri, J. J. Mason, J. K. McMaster, J. A. Miles, P. T. Mitchell, J. D. Murphree, N. A. Neff-Mallon, T. Oh, V. Omole, C. P. Simon, N. Pederson, M. A. Perlin, A. Reiter, R. Rines, P. Romlow, A. M. Scott, D. Stiefvater, J. R. Tanner, A. K. Tucker, I. V. Vinogradov, M. L. Warter, M. Yeo, M. Saffman, and T. W. Noel, Universal neutral-atom quantum computer with individual optical addressing and nondestructive readout, *PRX Quantum* **6**, 030334 (2025).

[13] R. B.-S. Tsai, X. Sun, A. L. Shaw, R. Finkelstein, and M. Endres, Benchmarking and fidelity response theory of high-fidelity Rydberg entangling gates, *PRX Quantum* **6**, 010331 (2025).

[14] M. Peper, Y. Li, D. Y. Knapp, M. Bileska, S. Ma, G. Liu, P. Peng, B. Zhang, S. P. Horvath, A. P. Burgers, and J. D. Thompson, Spectroscopy and modeling of ^{171}Yb Rydberg states for high-fidelity two-qubit gates, *Phys. Rev. X* **15**, 011009 (2025).

[15] J. A. Muniz, M. Stone, D. T. Stack, M. Jaffe, J. M. Kindem, L. Wadleigh, E. Zalys-Geller, X. Zhang, C.-A. Chen, M. A. Norcia, J. Epstein, E. Halperin, F. Hummel, T. Wilkason, M. Li, K. Barnes, P. Battaglino, T. C. Bohdanowicz, G. Booth, A. Brown, M. O. Brown, W. B. Cairncross, K. Cassella, R. Coxe, D. Crow, M. Feldkamp, C. Griger, A. Heinz, A. M. W. Jones, H. Kim, J. King, K. Kotru, J. Lauigan, J. Marjanovic, E. Megidish, M. Meredith, M. McDonald, R. Morshed, S. Narayanaswami, C. Nishiguchi, T. Paule, K. A. Pawlak, K. L. Pudenz, D. R. Pérez, A. Ryou, J. Simon, A. Smull, M. Urbanek, R. J. M. van de Veerdonk, Z. Vendeiro, T.-Y. Wu, X. Xie, and B. J. Bloom, High-fidelity universal gates in the ^{171}Yb ground-state nuclear-spin qubit, *PRX Quantum* **6**, 020334 (2025).

[16] A. Senoo, A. Baumgärtner, J. W. Lis, G. M. Vaidya, Z. Zeng, G. Giudici, H. Pichler, and A. M. Kauffman, High-fidelity entanglement and coherent multi-qubit mapping in an atom array, [arXiv:2506.13632](https://arxiv.org/abs/2506.13632) (2025).

[17] C. Poole, T. M. Graham, M. A. Perlin, M. Otten, and M. Saffman, Architecture for fast implementation of quantum low-density parity-check codes with optimized Rydberg gates, *Phys. Rev. A* **111**, 022433 (2025).

[18] L. Pecorari, S. Jandura, G. K. Brennen, and G. Pupillo, High-rate quantum LDPC codes for long-range-connected neutral atom registers, *Nat. Commun.* **16**, 1111 (2025).

[19] M. Saffman, T. G. Walker, and K. Mølmer, Quantum information with Rydberg atoms, *Rev. Mod. Phys.* **82**, 2313 (2010).

[20] J. H. Wesenberg, K. Mølmer, L. Rippe, and S. Kröll, Scalable designs for quantum computing with rare-earth-ion-doped crystals, *Phys. Rev. A* **75**, 012304 (2007).

[21] G. Doulsinos, A. Delakouras, and D. Petrosyan, Fundamental bound on entanglement generation between interacting Rydberg atoms, [arXiv:2512.13379](https://arxiv.org/abs/2512.13379) (2025).

[22] T. Graham, M. Kwon, B. Grinkemeyer, A. Marra, X. Jiang, M. Lichtman, Y. Sun, M. Ebert, and M. Saffman, Rydberg mediated entanglement in a two-dimensional neutral atom qubit array, *Phys. Rev. Lett.* **123**, 230501 (2019).

[23] X. L. Zhang, A. T. Gill, L. Isenhower, T. G. Walker, and M. Saffman, Fidelity of a Rydberg blockade quantum gate from simulated quantum process tomography, *Phys. Rev. A* **85**, 042310 (2012).

[24] L. S. Theis, F. Motzoi, F. K. Wilhelm, and M. Saffman, A high fidelity Rydberg blockade entangling gate using shaped, analytic pulses, *Phys. Rev. A* **94**, 032306 (2016).

[25] A. Mitra, S. Omanakuttan, M. J. Martin, G. W. Biedermann, and I. H. Deutsch, Neutral-atom entanglement using adiabatic rydberg dressing, *Phys. Rev. A* **107**, 062609 (2023).

[26] N. Khaneja, T. Reiss, C. Kehlet, T. Schulte-Herbrüggen, and S. J. Glaser, Optimal control of coupled spin dynamics: design of nmr pulse sequences by gradient ascent algorithms, *Journal of magnetic resonance* **172**, 296 (2005).

[27] V. Buchemavari, S. Omanakuttan, Y.-Y. Jau, and I. Deutsch, Quantum control of qudits encoded in Rydberg ensembles (2025), [In preparation](https://arxiv.org/abs/2506.13632).

[28] V. Buchemavari, S. Omanakuttan, Y.-Y. Jau, and I. Deutsch, Entangling quantum logic gates in neutral atoms via the microwave-driven spin-flip blockade, *Phys. Rev. A* **109**, 012615 (2024).

[29] G. Giudici, S. Veroni, G. Giudice, H. Pichler, and J. Zeiher, Fast entangling gates for Rydberg atoms via resonant dipole-dipole interaction, *PRX Quantum* **6**, 030308 (2025).

[30] I. I. Beterov, I. I. Ryabtsev, D. B. Tretyakov, and V. M. Entin, Quasiclassical calculations of blackbody-radiation-induced depopulation rates and effective lifetimes of Rydberg nS, nP, and nD alkali-metal atoms with $n \leq 80$, *Phys. Rev. A* **79**, 052504 (2009).

[31] B. E. Anderson, H. Sosa-Martinez, C. A. Riofrío, I. H. Deutsch, and P. S. Jessen, Accurate and robust unitary transformations of a high-dimensional quantum system, *Phys. Rev. Lett.* **114**, 240401 (2015).

[32] D. Petrosyan, F. Motzoi, M. Saffman, and K. Mølmer, High-fidelity Rydberg quantum gate via a two-atom dark state, *Phys. Rev. A* **96**, 042306 (2017).

[33] M. Saffman, Quantum computing with atomic qubit arrays: confronting the cost of connectivity, [arXiv:2505.11218](https://arxiv.org/abs/2505.11218) (2025).

[34] D. C. Cole, E. Copenhaver, G. T. Hickman, D. Mason, W. C. Chung, and M. T. Lichtman, Demonstration of a fast $\pi - 2\pi - \pi$ Rydberg entangling gate for finite blockade, in *Proc. of 54th DAMOP meeting* (2023) p. U09.00006.